


SUPERMAN regulates floral whorl boundaries through control of auxin biosynthesis

Yifeng Xu^{1,2}, Nathanaël Prunet^{3,4,5}, Eng-Seng Gan¹, Yanbin Wang¹, Darragh Stewart⁶, Frank Wellmer^{3,6}, Jiangbo Huang^{1,7}, Nobutoshi Yamaguchi^{2,8}, Yoshitaka Tatsumi², Mikiko Kojima^{8,9}, Takatoshi Kiba^{8,9}, Hitoshi Sakakibara^{8,9}, Thomas P Jack⁵, Elliot M Meyerowitz^{3,4} & Toshiro Ito^{1,2,3,7,*} 

Abstract

Proper floral patterning, including the number and position of floral organs in most plant species, is tightly controlled by the precise regulation of the persistence and size of floral meristems (FMs). In *Arabidopsis*, two known feedback pathways, one composed of WUSCHEL (WUS) and CLAVATA3 (CLV3) and the other composed of AGAMOUS (AG) and WUS, spatially and temporally control floral stem cells, respectively. However, mounting evidence suggests that other factors, including phytohormones, are also involved in floral meristem regulation. Here, we show that the boundary gene *SUPERMAN* (*SUP*) bridges floral organogenesis and floral meristem determinacy in another pathway that involves auxin signaling. *SUP* interacts with components of polycomb repressive complex 2 (PRC2) and fine-tunes local auxin signaling by negatively regulating the expression of the auxin biosynthesis genes *YUCCA1/4* (*YUC1/4*). In *sup* mutants, derepressed local *YUC1/4* activity elevates auxin levels at the boundary between whorls 3 and 4, which leads to an increase in the number and the prolonged maintenance of floral stem cells, and consequently an increase in the number of reproductive organs. Our work presents a new floral meristem regulatory mechanism, in which *SUP*, a boundary gene, coordinates floral organogenesis and floral meristem size through fine-tuning auxin biosynthesis.

Keywords auxin; floral meristem; floral organogenesis; H3K27me3; polycomb repressive complexes; SUPERMAN

Subject Categories Plant Biology

DOI 10.15252/embj.201797499 | Received 4 June 2017 | Revised 25 March 2018 | Accepted 4 April 2018 | Published online 15 May 2018

The EMBO Journal (2018) 37: e97499

Introduction

In many angiosperms, floral patterning is tightly controlled by the precise coordination of stem cell proliferation in the floral meristem (FM), commitment of stem cell descendants to specific floral organs, and establishment of meristem-to-organ and organ-to-organ boundaries. By such mechanisms, the number and position of floral organs for a given species are well defined. Wild-type (WT) *Arabidopsis* flowers consist of four types of organs arranged in a series of concentric whorls: four sepals in the outermost whorl 1, followed by four petals in whorl 2, six stamens in whorl 3, and two fused carpels in the innermost whorl 4. While three classes of homeotic genes, classes A, B, and C, function alone or in combination to determine the cell identities of floral organs (Bowman *et al*, 1991; Coen & Meyerowitz, 1991), the precise developmental regulations of the FM that determine the family- and/or species-specific numbers of floral organs and whorls remain unknown.

In *Arabidopsis*, a negative feedback loop between the *WUSCHEL* (*WUS*)-expressing organizing center and *CLAVATA3* (*CLV3*)-expressing stem cells maintains the appropriate size of both FMs and shoot apical meristems (SAMs; Brand *et al*, 2000). FM activity is associated with the number of floral organs. Mutation in *WUS* causes plants to lose the ability to maintain stem cells and prematurely stops organ formation (Laux *et al*, 1996). In contrast, stem cells accumulate in *clv3* mutants due to unrestricted *WUS* expression, leading to the formation of more organs (Clark *et al*, 1995; Fletcher *et al*, 1999). Unlike the indeterminate SAM, the FM is determinate and ceases to maintain stem cells after the initiation of carpels. Another negative feedback between *WUS* and the class C gene *AGAMOUS* (*AG*) plays a central role in this termination process (Lenhard *et al*, 2001; Lohmann *et al*, 2001; Sun *et al*, 2009, 2014). *AG* is induced at floral stage 3 by *WUS* and the FM regulator *LEAFY* (*LFY*) in whorls 3 and 4 of floral primordia where stamens and

1 Temasek Life Sciences Laboratory (TLL), National University of Singapore, Singapore, Singapore

2 Plant Stem Cell Regulation and Floral Patterning Laboratory, Biological Science, Nara Institute of Science and Technology, Ikoma, Nara, Japan

3 Division of Biology and Biological Engineering, California Institute of Technology, Pasadena, CA, USA

4 Howard Hughes Medical Institute, California Institute of Technology, Pasadena, CA, USA

5 Department of Biological Sciences, Dartmouth College, Hanover, NH, USA

6 Smurfit Institute of Genetics, Trinity College Dublin, Dublin 2, Ireland

7 Department of Biological Sciences, Faculty of Science, National University of Singapore, Singapore, Singapore

8 Precursory Research for Embryonic Science and Technology, Japan Science and Technology Agency, Kawaguchi-shi, Saitama, Japan

9 RIKEN Center for Sustainable Resource Science, Yokohama, Japan

*Corresponding author. Tel: +81 0743 72 5500; Fax: +81 0743 72 5500; E-mail: itot@bs.naist.jp

carpels will develop in later stages (Lohmann *et al*, 2001). *AG* in turn represses *WUS*, both directly by affecting the recruitment of polycomb group (PcG) proteins to the *WUS* locus and indirectly through the C2H2 zinc finger protein KNUCKLES (KNU), to terminate stem cell maintenance at floral stage 6, approximately 2 days after *AG* induction (Sun *et al*, 2009; Liu *et al*, 2011). In *ag* and *knu* loss-of-function mutants, *WUS* expression remains active beyond stage 6, which is sufficient to induce FM indeterminacy, leading to the production of extra whorls of reproductive organs (Lenhard *et al*, 2001; Sun *et al*, 2009). *AG* also activates the YABBY family transcription factor CRABS CLAW to regulate carpel organogenesis and FM determinacy through the establishment of auxin maxima in the fourth whorl (Yamaguchi *et al*, 2017).

The number and position of floral organs are also controlled by boundary genes, which function through various mechanisms, including the crosstalk with the phytohormone auxin (Zadnikova & Simon, 2014). The NAC family transcription factors *CUP-SHAPED COTYLEDON1-3* (*CUC1-3*), which participate in the formation of boundaries between organs and between organs and meristems, are negatively regulated by auxin-dependent signaling pathways (Takada *et al*, 2001; Daimon *et al*, 2003). In the *Arabidopsis* SAM, new floral primordia are initiated in the peripheral zone, at the region where auxin concentration is highest. As the primordium forms, auxin is depleted from the boundary separating the emerging primordium from the meristem and flows toward the incipient position of the next primordium (Heisler *et al*, 2005). Thus, *CUC* genes are restricted in the boundary regions of low auxin activity. Auxin also controls the size of the root meristem non-cell autonomously; this auxin signaling is antagonistic to cytokinin signaling, and cytokinin negatively controls the root meristem size (Dello Ioio *et al*, 2007). In contrast to root meristems, cytokinin signaling and *WUS* activity in the SAM could reinforce each other in a positive feedback (Leibfried *et al*, 2005; Gordon *et al*, 2009; Zhao *et al*, 2010). Although auxin and cytokinin show opposite functions in the regulation of shoot and root meristems, the function of auxin in FMs is not well understood (Werner *et al*, 2003; Schaller *et al*, 2015).

The *SUPERMAN* (*SUP*) gene encodes a transcription factor with a C2H2-type zinc finger motif and is proposed to function as a boundary gene to separate the stamen-producing whorl 3 from the carpel-producing whorl 4 (Sakai *et al*, 1995). Loss of function of *SUP* leads to an increased number of stamens, suggesting that *SUP* is involved in both floral patterning and FM determinacy (Bowman *et al*, 1992; Gaiser *et al*, 1995). *AG* is a positive regulator of *SUP* transcription, and *SUP* mRNA level is greatly reduced in *ag* mutants (Bowman *et al*, 1992). Notably, the transient and weak expression of *SUP* in *ag* mutants is sufficient for some level of function, since *ag sup* double mutants show strong synergistic effects on FM size, causing enlarged and fasciated FMs (Bowman *et al*, 1992). Although *sup* mutants were identified and well characterized decades ago, how *SUP* functions to bridge floral organogenesis and FM determinacy is still unclear. A recent study showed that *SUP* cell autonomously prevents the ectopic expression of class B/stamen identity genes in whorl 4, and non-cell autonomously promotes stem cell termination in developing flowers (Prunet *et al*, 2017). The ectopic expression of *SUP* in different plant species leads to dwarf plants with organs of reduced size, which could be associated with both auxin and cytokinin signaling defects (Hiratsu

et al, 2002; Nibau *et al*, 2011). However, it is difficult to distinguish the causal factors of the *sup* phenotypes from the consequence of altered morphology.

Here, we elucidate how *SUP* functions to control floral organogenesis and FM size non-cell autonomously. *SUP* interacts with PcG proteins to exert its function as an active repressor and negatively regulates auxin biosynthesis in the stamen-to-carpel boundary region. In the *sup* mutant, the derepression of *YUCCA* (*YUC*) genes *YUC1* and *YUC4* leads to increased auxin accumulation and the formation of extra primordia of reproductive organs. Consistently, treatment with an anti-auxin (*p*-chlorophenoxyisobutyric acid, PCIB) can rescue the stamen number and carpel defects of *sup* mutants. Increased local auxin biosynthesis in the *SUP*-expressing region leads to *sup*-like floral phenotypes. Our work presents a new mechanism on how the boundary gene *SUP* coordinates floral organogenesis and FM size through fine-tuning of auxin biosynthesis.

Results

SUP regulates floral stem cells non-cell autonomously

We first tested whether the formation of supernumerary stamens in *sup* mutants is associated with *WUS* function in FMs. A loss of *WUS* activity leads to the premature termination of FMs so that both *wus-1* single-mutant and *wus-1 sup-5* double-mutant flowers typically form only a single stamen and no carpels (Laux *et al*, 1996; Fig 1A and B). Thus, *wus-1* is fully epistatic to *sup*, suggesting that the *sup* phenotype of supernumerary stamens is

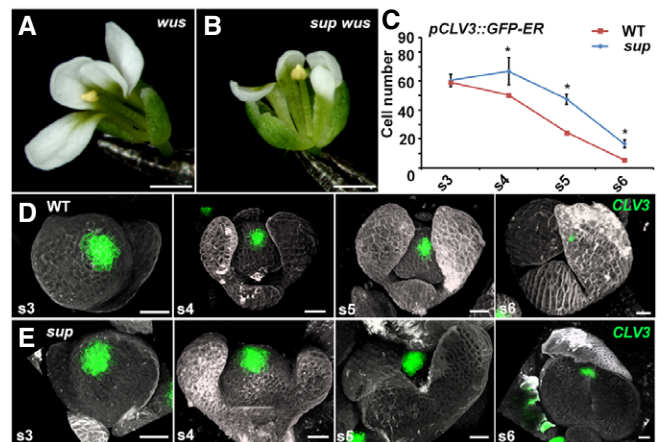


Figure 1. *SUP* spatially controls the FM size in a non-cell-autonomous manner.

- A, B *wus-1* (A) and *sup-5 wus-1* (B) mutant flowers with one stamen and without carpels. Scale bars, 1 mm.
- C The comparison of the number of cells with the stem cell marker *pCLV3::GFP-ER* signals in WT and *sup-5*. The numbers of cells with the signals were counted based on the z-stack images. From stage 4 (s4) onwards, the *sup-5* floral buds showed increased numbers of *CLV3*-expressing stem cells compared with those of WT. Error bars indicate s.d. of 12–15 samples; two-tailed Student's *t*-test, **P* < 0.05.
- D, E The *pCLV3::GFP-ER* (green) in WT (D) and *sup-5* (E) floral buds at different floral stages. Scale bars, 20 μ m.

dependent on *WUS* function. In contrast, flowers of *ag-1 sup-5* double mutants show enhanced meristem indeterminacy (Bowman *et al*, 1991; Uemura *et al*, 2017). Taken together, these results suggest that SUP may regulate *WUS* in FMs and that this regulation might be at least in part independent from the known AG-*WUS* feedback pathways.

To address whether SUP regulates floral stem cell activities, we monitored the expression of the stem cell marker *CLV3* in *sup-5* mutant flowers (Fig 1C–E). Using a *pCLV3::GFP-ER* reporter (Reddy & Meyerowitz, 2005), we determined that there is no obvious difference of fluorescence intensity between WT and *sup*; however, the *CLV3* expression region appeared slightly broader in *sup* flowers from stage 4 onward (Fig 1D and E). To further test this, we counted the number of cells expressing *pCLV3::GFP-ER* in *sup* and WT flowers at different stages and found that while the number of cells expressing *pCLV3::GFP-ER* was comparable between WT and *sup* at stage 3, from stage 4 onward, it was significantly higher in *sup* floral buds (Fig 1C–E). This result suggests that there are an increased number of floral stem cells in *sup* mutants. To confirm this observation, we employed a floral induction system (denoted: *ap1 cal p35S::API-GR*), which is based on the activation of a fusion protein between the APETALA1 (*AP1*) transcription factor and the steroid-binding domain of the rat glucocorticoid receptor (GR) in the inflorescence-like meristems of *ap1 cauliflower (cal)* double mutants by dexamethasone (DEX) treatment and allows the collection of a large number of synchronized floral buds for analysis (Wellmer *et al*, 2006). Using real-time quantitative reverse transcription PCR (qRT-PCR), we detected increased transcription levels for both *CLV3* and *WUS* in stage 6 flowers of *ap1 cal p35S::API-GR sup-5* plants relative to those of *ap1 cal p35S::API-GR* plants (Fig EV1A). We also detected *pCLV3::GFP-ER* expression at later floral stages in *sup-5* than in the wild type (Fig EV1B), confirming previous reports that floral stem cell termination is delayed in *sup* (Prunet *et al*, 2017). Altogether, our data show that SUP influences floral stem cells both spatially and temporally.

We also analyzed the expression of the meristem marker SHOOT MERISTEMLESS (*STM*) by using a translational reporter *pSTM::STM-VENUS* and a transcriptional reporter *pSTM::CFP-N7* (Fig EV2; Heisler *et al*, 2005; Landrein *et al*, 2015). Up to stage 4, *STM* expression appears identical in *sup-5* and WT flowers: *STM* is initially expressed throughout stage 1–2 flower buds, before fading from developing sepals at stage 3 (Fig EV2A and B). *STM* expression domain appears larger in *sup* than in the wild type at late stage 5 (Fig EV2A and B), which is associated with an enlarged FM in *sup*. By stage 6, *STM* expression ceases in whorls 2 and 3 in both wild-type and *sup-5* flowers (Fig EV2A and B). *STM* then becomes restricted to emerging carpel primordia in the fourth whorl of wild-type flowers, whereas in *sup-5* flowers, its expression domain in the center becomes enlarged. Later on, *STM* only remains expressed at the carpel margins/placenta region in the WT (Fig EV2C and D). Conversely, in *sup-5*, *STM* is expressed in a larger domain, which encompasses the FM that keeps proliferating; *STM* is also transiently expressed in the emerging extra stamen primordia that form in the center of *sup-5* flowers (Fig EV2C and D). The expression domain of SUP forms a ring at the boundary between whorls 3 and 4 (Appendix Fig S1A and B) that is mostly non-overlapping with that of *CLV3* or *WUS* throughout flower development, indicating that

SUP affects floral stem cells non-cell autonomously (Prunet *et al*, 2017).

Auxin signaling is disrupted in *sup* mutants

To investigate how SUP regulates organ boundaries, FM size, and differentiation, we compared the expression of a *CUC2* reporter in wild-type and *sup* flowers. *CUC* genes encode closely related members of the NAC family of transcription factors, which participate in shoot meristem and boundary formation (Takada *et al*, 2001; Daimon *et al*, 2003). *In situ* hybridization analysis showed *CUC2* mRNA accumulation in the center of FMs in *sup-1* (Breuil-Broyer *et al*, 2004). As ectopic expression of *CUC2* is associated with an increased number of petals (Huang *et al*, 2012), we monitored *CUC2* expression using *pCUC2::CUC2-3xVENUS-N7* (Heisler *et al*, 2005) in the *sup* mutant (Fig EV3A–D). *CUC2* is widely expressed in stage 3 floral buds in both WT and *sup* (Fig EV3A and B). From stage 4 onward, clear differences in *CUC2* expression were observed between WT and *sup* flowers. In the WT, high *CUC2* expression was observed in cells at the boundary regions between the sepal primordia, and in the inner part of the whorl 3/4 boundary regions, while the central region of the FM showed no *CUC2* expression (Fig EV3A and C). In *sup*, *CUC2* expression was also observed in the FM region (Fig EV3B and D), in a domain where SUP is not normally expressed, suggesting that *CUC2* is not a direct target of SUP. Since it has been shown that *CUC2* is induced by low levels of auxin but repressed by high levels of auxin (Heisler *et al*, 2005), we hypothesized that auxin signaling or accumulation could be disturbed in *sup* mutant flowers. To test this hypothesis, we monitored the activity of the auxin response reporters *pDR5rev::2xGFP-N7* and *pDR5rev::GFP-ER* in *sup* and WT flowers (Xu *et al*, 2006a; Liao *et al*, 2015). In WT stage 4 flower buds, *DR5* expression occurs only at the sites of petal primordia initiation and at the tips of sepals (Fig 2A and Appendix Fig S2A). In contrast, in *sup* mutant stage 4 flower buds, *DR5* is also expressed at the whorl 3/4 boundary, indicating an increase in auxin response in that region (Fig 2B and Appendix Fig S2B). The DII-VENUS auxin sensor, expressed under the control of the ubiquitous *RPS5A* promoter, is degraded in presence of auxin (Liao *et al*, 2015). In WT flower buds at stage 4, DII-VENUS is detected at the boundary between whorls 3 and 4 but not in the center of the flower, indicating that auxin is depleted at the boundary, but not in the FM region (Fig 2C). In contrast, in *sup* flower buds at stage 4, DII-VENUS is observed in the center of the FM but not at the boundary between whorls 3 and 4, showing that auxin is depleted in the FM region rather than at the boundary (Fig 2D). These data imply that the loss of SUP function leads to auxin accumulation, rather than depletion, at the boundary between whorl 3 and 4, and to a reduction in auxin in the center of the FM. The increase in auxin at the whorl 3/4 boundary in *sup* could be due either to an increase in auxin biosynthesis or to a perturbation of auxin transport. To test whether the *sup* phenotype is due to the cell-autonomous effect of an increase in auxin levels or due to perturbed auxin transport, we treated *sup* mutant inflorescences with *p*-chlorophenoxyisobutyric acid (PCIB), which inhibits auxin action (Oono *et al*, 2003). PCIB treatment strongly rescued both the stamen number and carpel defects in *sup-5* (Fig 2E–G). Next, we tested the

stage-specific rescue effect of PCIB by measuring time to anthesis. Generally, stage 4–5 floral buds were rescued better than stage 6 floral buds in terms of carpel morphology and stamen numbers (Fig 2G). We also tested the effect of PCIB treatment on *CUC2* and *DR5* expressions in *sup* (Fig EV4). *CUC2* expression was not reversed to a WT-like pattern following treatment with PCIB. Instead, *CUC2* was ectopically expressed through most of the flower bud (Fig EV4A and B), which may be due to *CUC2* activation by low auxin levels. In contrast, *DR5* expression at the whorl 3/4 boundary is almost completely absent in *sup* flowers 5 h after

PCIB treatment (Fig EV4C and D), indicating that PCIB restores a wild-type pattern of auxin response in *sup* flowers, which is consistent with the fact that PCIB treatments rescue the *sup* phenotype (Fig 2E–G).

To test whether an increase in auxin levels in the *SUP* expression domain is sufficient to cause the development of supernumerary stamens and carpel defects, we generated the transgenic line *pSUP::iaaH* with the bacterial auxin biosynthetic gene *iaaH* under the control of the *SUP* regulatory regions. *iaaH* can convert the auxin precursor, indoleacetamide (IAM) to the active form of auxin,

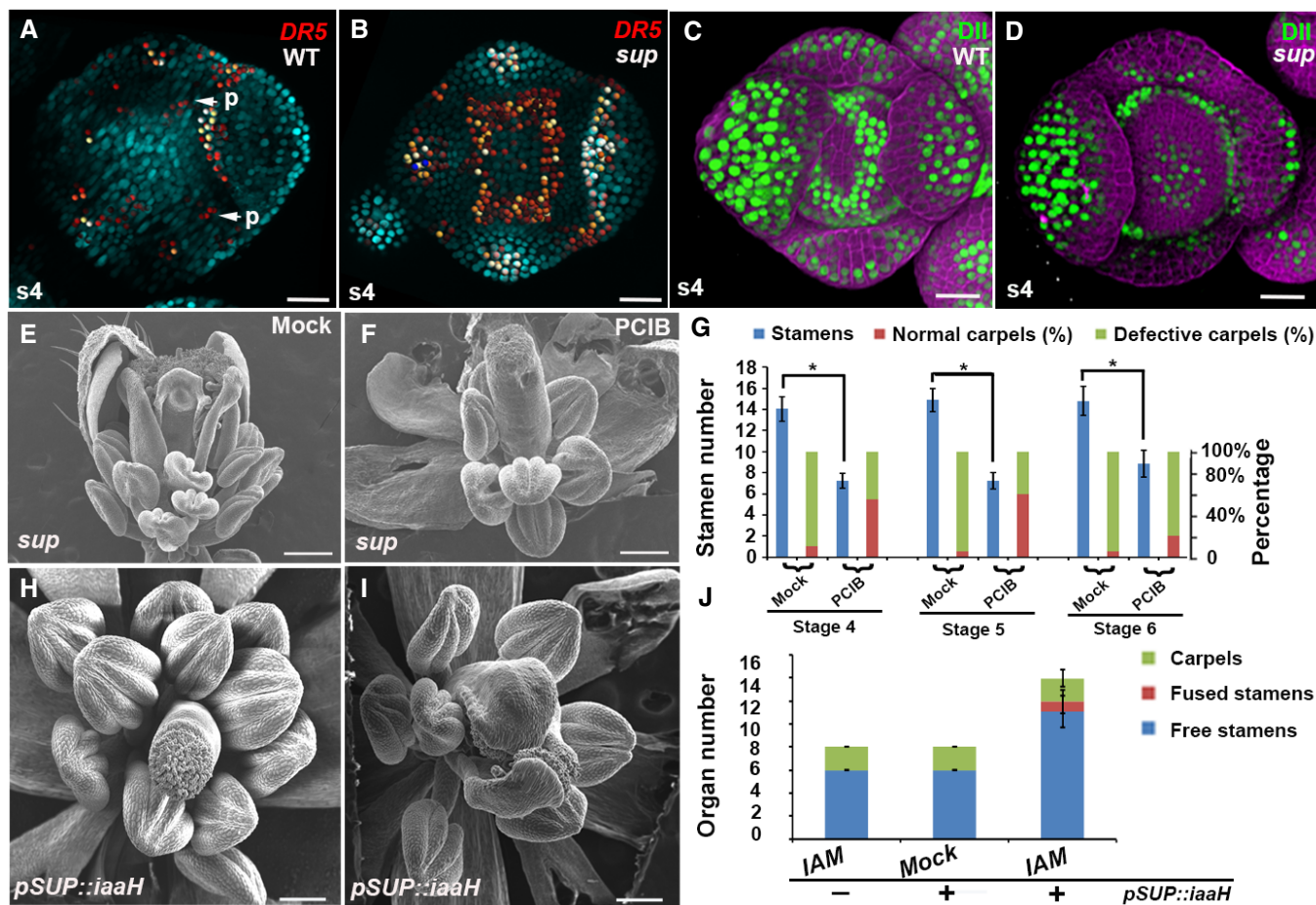


Figure 2. *sup* mutant phenotypes are associated with perturbed auxin distribution.

- A, B Activity of the auxin marker *pDR5rev::2xGFP-N7* in stage 4 (s4) floral buds of WT (A) and *sup-1* (B). In WT flowers, the fluorescence signal was detected mostly at the tips of the sepals and at the sites (p, marked with the arrows) where the petal primordia would emerge at later stages (A). In *sup-1* flowers, strong reporter activity was additionally detected at the whorl 3/4 boundary.
- C, D Activity of the auxin reporter DII-VENUS (green) in stage 4 floral buds of WT (C) and *sup-1* (D). In WT flowers, fluorescence signals were detected at the whorl 3/4 boundary but were absent at the center of the FM and the tips of the sepals (C). In contrast, DII-VENUS signals were absent at the whorl 3/4 boundary but were detected in the FM region (D).
- E, F *sup-5* flowers after treatment with the anti-auxin PCIB (F) and mock solutions (E). While the mock treatment did not affect *sup-5* flowers (E), treatment with PCIB strongly rescued both carpels and stamen numbers.
- G The statistical analysis indicated that PCIB treatment strongly rescued stage 4–5 floral buds, which took approximately 9–10 days to anthesis; the floral buds of stage 6 were best rescued in terms of carpel morphology. Error bars indicate s.d. of 20 flowers from around 10 individual plants; two-tailed Student's t-test, * $P < 0.05$.
- H–J *pSUP::iaaH* transgenic flowers with the IAM treatment mimicked the various *sup*-like phenotypes, including increased stamen numbers and defective carpels, as shown in the SEM images of the flowers (H, I). Wild-type plants (lacking *pSUP::iaaH*) were treated with IAM as a negative control. The number of free stamen, fusion stamen, and carpels was determined for a total of 20 flowers from 20 individual plants and is summarized in (J). Error bars indicate s.d.

Data information: Scale bars, 20 μ m for (A–D), 200 μ m for (E, F, H, I).

indole-3-acetic acid (IAA) in *Arabidopsis* (Oka et al, 1999). With a 1 mM IAM treatment, flowers of the transgenic plants showed weak to strong *sup*-like phenotypes. In contrast, WT flowers treated with IAM and mock-treated *pSUP::iaaH* flowers were unaffected (Fig 2H–J). These results confirmed that a local increase in auxin biosynthesis at the boundary region between the 3rd and 4th whorl is sufficient to cause *sup*-like phenotypes.

Auxin gradients and maxima rely on both local biosynthesis and polar transport. We therefore tested the effect of the polar auxin transport inhibitor N-1-naphthylphthalamic acid (NPA) on the *sup* mutant phenotype. The application of NPA at stages 4–6 partially rescued both carpel morphology and stamen number defects in *sup* (Appendix Fig S3), suggesting that polar auxin transport is also important for the expression of the *sup* phenotype.

Derepression of local auxin biosynthesis is responsible for *sup* mutant phenotypes

To identify the downstream targets of SUP that contribute to auxin biosynthesis and/or accumulation, we generated *p35S::SUP-GR* and *pSUP::SUP-GR* transgenes that allow the DEX-dependent activation of SUP when expressed under either the SUP promoter or ubiquitously with the enhancer element of the cauliflower mosaic virus 35S promoter inserted in the SUP promoter. After DEX treatment, we observed a complete rescue of the *sup-5* mutant phenotype in the *pSUP::SUP-GR* plants, indicating that SUP-GR mimics the endogenous function of SUP (Appendix Fig S4). *p35S::SUP-GR* plants showed reduced sizes of floral organs and increased carpel numbers (Appendix Fig S5). Once introduced into the *clv3* mutant (which forms larger meristems than the WT), ectopic SUP expression caused the differentiation of FMs into leaf-like structures in all the flowers observed (Appendix Fig S5). These results suggest that the function of SUP could be associated with organ differentiation.

To identify downstream targets of SUP at a genome-wide scale, we performed microarray analyses with RNA isolated from *p35S::SUP-GR* inflorescences 4 h after DEX and mock treatments. In these experiments, we identified 642 down-regulated and 421 up-regulated genes whose expression changed more than twofold after DEX treatment (Gene Expression Omnibus accession number GSE92729). While there was no significant enrichment of Gene Ontology (GO) terms among up-regulated genes, for the down-regulated genes, eight GO terms were over-represented, which were classified into three superclusters based on their relatedness using REVIGO (Supek et al, 2011), including “hormone metabolism” and “response to endogenous stimulus” (Fig 3A). Our reporter assays as well as a previous study (Nibau et al, 2011) suggest that SUP may function in the auxin signaling pathway. Thus, the supercluster of “hormone metabolism”, which contains three hormone-related GO biological processes: hormone metabolism, $P_{\text{FDR}} = 0.00039$; regulation of hormone level, $P_{\text{FDR}} = 0.0011$; auxin biosynthesis, $P_{\text{FDR}} = 0.0042$ (Fig 3A), was further inspected. There are total 17 genes in the category of “hormone metabolism”. Among these, 12 of the genes also belong to the category of “regulation of hormone level”, and interestingly, eight of which are listed in the term of “auxin synthesis” as well (Appendix Table S1). These eight genes include three known auxin biosynthesis genes: the YUCCA (*YUC*) flavin monooxygenases *YUC1/4* and the TRP-a-transferase TRYPTOPHAN AMINOTRANSFERASE RELATED 2

(*TAR2*) (Appendix Table S1). In addition, two auxin efflux transporters, *PIN-FORMED1/3* (*PIN1/3*), were also identified among the down-regulated genes (Appendix Table S1). We confirmed these microarray results by analyzed RNA levels in *p35S::SUP-GR* at 2 and 4 h after DEX treatment using qRT-PCR (Fig 3B). To further test whether these four genes are targets of SUP, we also compared their expression levels in stage 4 floral buds of the WT and *sup* mutants using the *ap1 cal p35S::API-GR* floral induction system (Wellmer et al, 2006). As SUP is a strong active repressor (Hiratsu et al, 2002), we expected to see increased transcription levels of its direct targets in *sup* compared with those in WT. The transcription of *YUC1/4* was up-regulated in *sup* at approximately stage 4 (3 days after DEX treatment; Fig 3C). In contrast, *PIN3/4* were down-regulated in *sup* (Fig 3C), which may be due to an indirect feedback regulation. These expression comparisons suggest that auxin biosynthesis genes may be immediate targets of SUP and that their derepression is primarily responsible for the *sup* mutant phenotype.

To test whether the increased expression of YUC flavin monooxygenases in *sup* leads to an over-accumulation of auxin, we again employed the floral induction system to measure the major form of auxin IAA in WT and *sup* mutant flowers (Fig 3D). While in mock-treated inflorescences before the initiation of flower formation, we did not detect any significant difference, IAA levels in stage 4 *sup* flowers were significantly ($P = 0.042$) higher than those in the WT (Fig 3D), in agreement with the observed derepression of *YUC1/4* genes.

SUP directly binds to *YUC1/4* genomic regions and mediates the deposition of the repressive mark H3K27me3

To test whether *YUC1/4* are direct SUP target genes, we analyzed the binding profiles of SUP-GFP at the *YUC1* and *YUC4* loci. As the spatial and temporal SUP-GFP protein expression domain is quite limited in *pSUP::SUP-GFP* (Appendix Fig S1B), we performed a ChIP binding assay with *pSUP::SUP-GFP* in *ap1 cal p35S::API-GR* to obtain a large amount of synchronized stage 4 floral buds. We detected enrichment of SUP-GFP at the 5'-proximal promoters and coding regions of both *YUC1* and *YUC4* compared with those of the control (Fig 4A, B, D, and E). It has been reported that the coding region of *INNER NO OUTER* (*INO*) is required for SUP regulation during ovule development (Meister et al, 2002), suggesting that it may not be unusual for SUP to bind the coding region of downstream targets.

Many genes involved in auxin synthesis and transport, including *YUC1/4*, are regulated by the polycomb group (PcG) complex, which can introduce an H3K27me3 repressive epigenetic mark to silence genes (Lafos et al, 2011). To address whether the repressive mark H3K27me3 is associated with transcriptional repression of SUP targets, we performed ChIP assays to look for differences in the H3K27me3 repressive mark and the H3K4me3 active mark in *ap1 cal p35S::API-GR* with or without the *sup* mutation at stage 4. The ChIP assay showed that H3K27me3 is reduced at both *YUC1* and *YUC4* loci in *sup* mutant floral buds (Fig 4A, C, D, and F), while H3K4me3 is increased (Appendix Fig S6), which is consistent with the transcriptional up-regulation of *YUC1/4*.

To investigate whether the SUP binding regions (including coding regions and introns) of *YUC1/4* are responsible for their

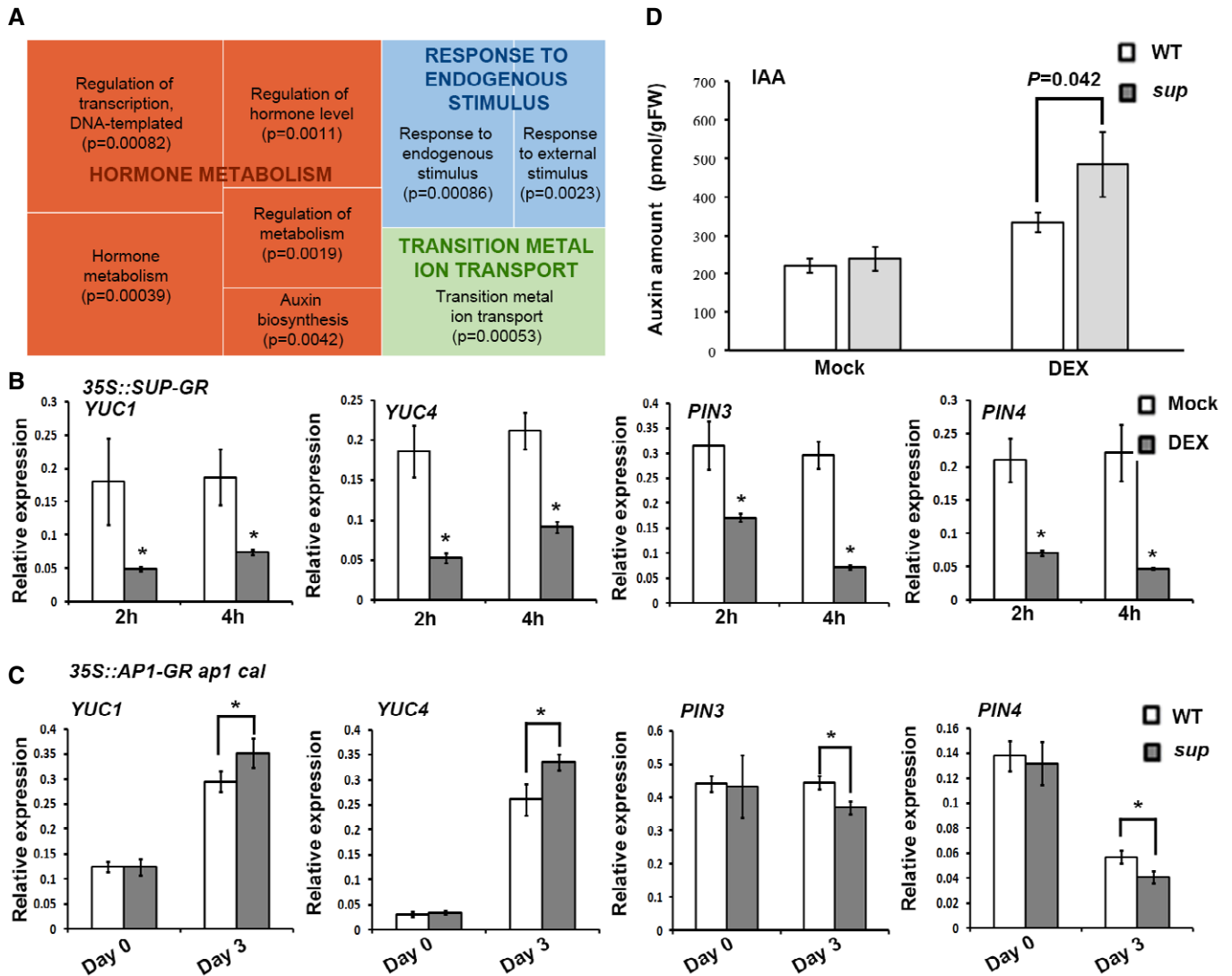


Figure 3. Increased auxin biosynthesis in the SUP-expressing region is essential for the *sup* mutant phenotype.

A REVIGO analysis of pathways significantly enriched among the down-regulated genes. Each rectangle is a single cluster representative for the non-redundant GO term, which are joined into "superclusters" of related terms, visualized with different colors. Size of the rectangles reflects the *P*-value.

B *YUC1/4* and *PIN3/4* are reduced in *35S::SUP-GR* inflorescences 2 and 4 h after treatment with 10 μ M DEX. Error bars indicate s.d. of three biological replicates; two-tailed Student's *t*-test, **P* < 0.05.

C Expression levels of *YUC1/4* and *PIN3/4* 3 days after 1 μ M DEX treatment in *ap1 cal p35S::API-GR sup-5* and *ap1 cal p35S::API-GR*. Expression of *YUC1/4* was increased in the *ap1 cal p35S::API-GR sup-5* background, while that of *PIN3/4* was reduced. Error bars indicate s.d. of three biological replicates; two-tailed Student's *t*-test, **P* < 0.05.

D IAA levels in *ap1 cal p35S::API-GR sup-5* and *ap1 cal p35S::API-GR* 3 days after treatment with 1 μ M DEX or a mock solution. The *P*-value was calculated using one-way ANOVA and standard errors from three biological replicates.

proper expression patterns in the inflorescence, we generated GUS reporters for *YUC1* and *4*, with and without the coding regions (Appendix Fig S7A–D). *YUC1*-GUS shows higher staining than that of *YUC4*-GUS, which is consistent with previous reports (Cheng et al, 2006). GUS staining is stronger and expands both spatially and temporally in the *pYUC1::GUS* and *pYUC4::GUS* lines compared to the full-length reporters *pYUC1::YUC1-GUS* and *pYUC4::YUC4-GUS* (Appendix Fig S7). qRT-PCR assays of *GUS* transcripts confirmed that the lower staining in *pYUC1::YUC1-GUS* and *pYUC4::YUC4-GUS* is mainly due to lower transcription of the transgenes

(Appendix Fig S7F). These data confirmed that the coding regions of *YUC1/4*, which are bound by SUP and contain high levels of H3K27me3, are important for their negative regulation (Fig 4A–F and Appendix Fig S7). However, the ectopic GUS expression observed in our transcriptional reporters is detected in sepals and is not exclusive to the whorl 3/4 boundary, suggesting that there are other regulators repressing *YUC1/4* via regulatory elements in the coding region of these genes (Appendix Fig S7). We could not see any obvious difference in GUS staining between the WT and *sup* with the *pYUC1::GUS* and *pYUC4::GUS* reporters (Fig EV5E–G).

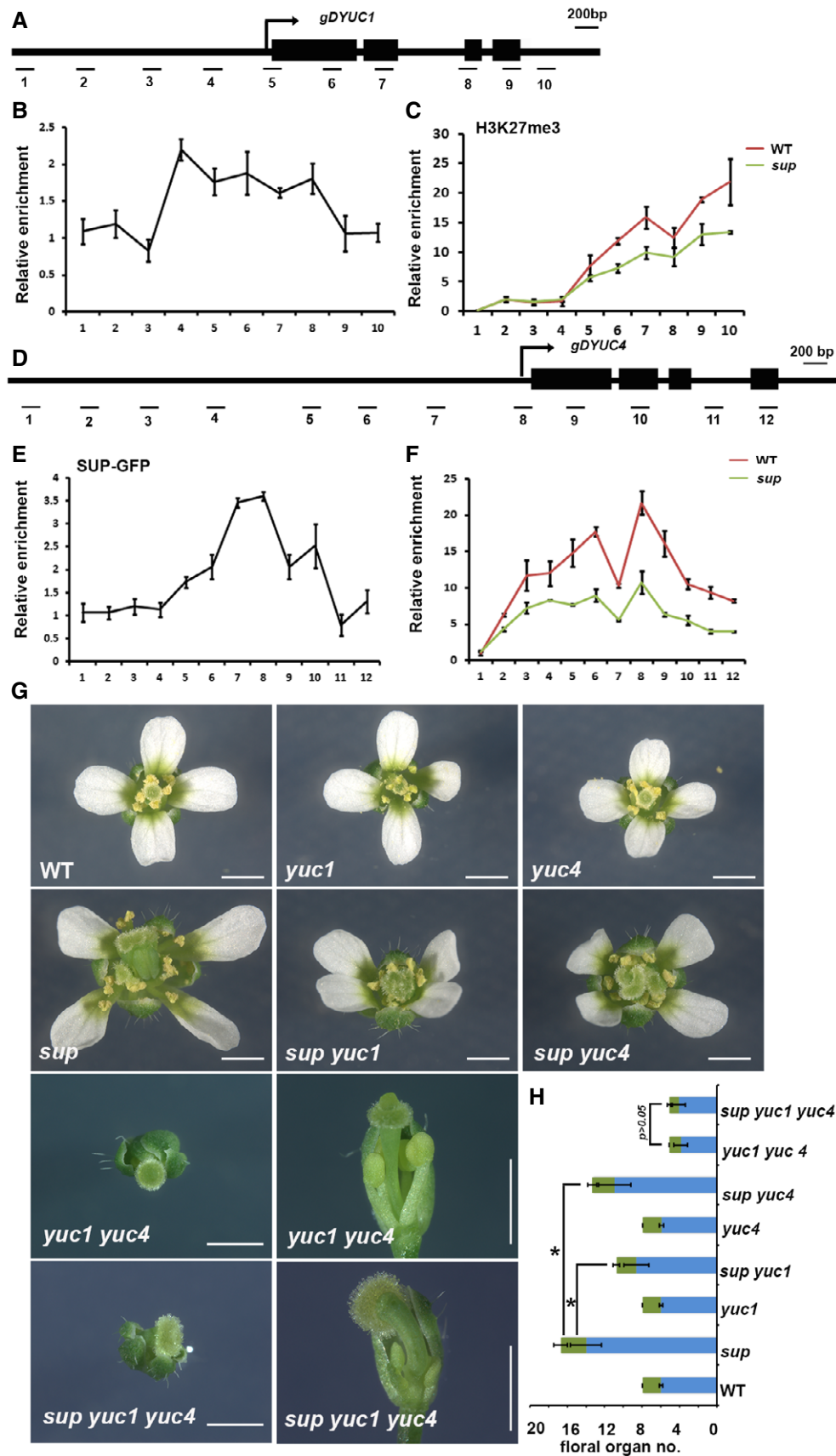


Figure 4.

Figure 4. SUP binds to YUC1/4 chromatin to achieve high levels of H3K27me3.

- A Schematic drawing of the *YUC1* genome structure showing regions amplified by primer sets used for ChIP analyses.
- B ChIP binding assay of the SUP protein at the *YUC1* genome. Relative enrichment of SUP-GFP at the *YUC1* locus, including the promoter and coding regions, was analyzed using the stage 4 floral buds from *ap1 cal p35S::AP1-GR sup-5 pSUP::SUP-GFP* plants.
- C Relative enrichment of H3K27me3 at the *YUC1* locus is decreased in the stage 4 floral buds of *ap1 cal p35S::AP1-GR sup-5* plants relative to *ap1 cal p35S::AP1-GR*.
- D Schematic drawing of the *YUC4* gene structure showing regions amplified by primers used for ChIP analyses.
- E ChIP binding assay of the SUP protein at the *YUC4* gene. Relative enrichment of SUP-GFP at the *YUC4* locus, including the promoter and coding regions, analyzed using the stage 4 floral buds of *ap1 cal p35S::AP1-GR sup-5 pSUP::SUP-GFP*.
- F Relative enrichment of H3K27me3 is decreased at the *YUC4* locus in stage 4 floral buds of *ap1 cal p35S::AP1-GR sup-5* compared with that of the WT control. Error bars represent standard errors with three biological repeats.
- G *yuc1* and *yuc4* mutant alleles partially rescue the stamen and carpel number defects of *sup-5*, while *yuc1 yuc4* is epistatic to *sup-5*. The *yuc4* mutation results in reduced floral organ size while *yuc4* appears WT-like. Both *yuc1* and *yuc4* single mutant have no defects in floral organ numbers. The *yuc1 yuc4* double mutant shows strong floral defects, namely a decreased numbers of stamen and carpel together with a reduction in floral organ size. The *sup-5 yuc1 yuc4* triple mutant shows a *yuc1 yuc4*-like floral morphology. A typical flower is shown for WT, *yuc1 yuc4*, *sup-5*, *sup-5 yuc1*, *sup-5 yuc4*, *yuc1 yuc4*, and *sup-5 yuc1 yuc4*, respectively. For *yuc1 yuc4* and *sup-5 yuc1 yuc4*, the top view and side view are shown for the same flower. Scale bars: 1 mm.
- H The statistical analysis showed a reduction in total stamens and carpels in *sup-5 yuc1* (8.60 ± 1.33 for stamen, 2.13 ± 0.34 for carpel, $n = 30$), *sup-5 yuc4* (10.93 ± 1.74 for stamen, 2.4 ± 0.50 for carpel, $n = 30$) once compared with *sup-5* (14.00 ± 1.68 for stamen, 2.7 ± 0.75 for carpel, $n = 30$). * $P < 0.05$ based on Student's *t*-test. There is no significant difference between *yuc1 yuc4* (3.8 ± 0.77 for stamen, 1.25 ± 0.44 for carpel, $n = 20$) and *sup-5 yuc1 yuc4* (4.05 ± 0.70 for stamen, 1.05 ± 0.23 for carpel, $n = 19$) in floral organ number and floral organ size, $P > 0.05$ with a Student's *t*-test.
- Data information: In (B, C, E and F), error bars indicate s.e.m. of three biological replicates. In (H), error bars indicate s.d.

However, ectopic GUS staining was observed in a region that resembles SUP expression domain in *sup* flowers at stage 4 with both full-length *pYUC1::YUC1-GUS* and *pYUC4::YUC4-GUS* reporters, which confirms that SUP represses *YUC1/4* at the boundary between whorl 3 and 4 in a cell-autonomous fashion (Fig EV5A–D).

Since *YUC1* and *YUC4* are direct targets of SUP, we tested whether the activity of *YUC1* and *YUC4* is essential for the expression of the *sup* mutant phenotype. Flowers of the *yuc1* single mutant do not show any obvious morphological defect (Fig 4G; Cheng *et al*, 2006), while *yuc4* single-mutant flowers show a reduction in the size of all floral organs (Fig 4G), consistent with previous reports that *YUC4* is broadly expressed. However, in contrast to previous reports (Cheng *et al*, 2006), our *yuc4* allele (SALK_047083) did not exhibit any obvious decrease in floral organ numbers (Fig 4G and H). Flowers of the *yuc1 yuc4* double mutant have a much stronger phenotype, with a strong reduction in both stamen and carpel numbers, along with abnormally shaped carpels (Fig 4G and H; Cheng *et al*, 2006). We next generated *yuc1 sup* and *yuc4 sup* double mutants as well as *yuc1 yuc4 sup* triple mutant plants. As expected, both *yuc1* and *yuc4* can partially rescue the increase in stamen and carpel number in *sup*, and *yuc1* rescues *sup* to a greater extent than *yuc4* (Fig 4G and H). The *yuc1 yuc4* double mutant is epistatic to *sup* (Fig 4G and H), confirming that SUP controls stamen and carpel number through the repression of *YUC1/4*. We next checked *DR5* expression in *sup yuc1*. Consistent with the partial rescue of the *sup* phenotype by *yuc1*, we observed a strong reduction in *DR5* activity at the whorl 3/4 boundary in *sup yuc1* flowers (Appendix Fig S8A–C).

Since our pharmacological analyses using auxin signaling and auxin transport inhibitors showed that *sup* mutant phenotypes depend on both auxin biosynthesis and auxin transport, we also checked the expression pattern of the auxin efflux transporter PIN3 using the *pPIN3::PIN3-GFP* reporter. *PIN3* transcript is slightly lower in a *sup* background compared to the wild type (Fig 3C), and there is no obvious difference of expression pattern between *sup* and the wild type (Appendix Fig S9). Based on these results, we conclude that SUP primarily functions through the control of auxin biosynthesis.

SUP forms a repressor complex with the PcG components CLF and TFL2

SUP is an active repressor with a conserved EAR motif at its C-terminus (Hiratsu *et al*, 2002; Yun *et al*, 2002). However, how SUP executes its repressor function is still unknown. Given that the repressive mark H3K27me3 is increased at the *YUC1/4* loci after the loss of function of SUP (Fig 4A–F), we explored the link between SUP and the repressive H3K27me3 modifications by performing a yeast two-hybrid assay to examine the interaction of SUP with factors associated with repressive histone modifications, including CURLY LEAF (CLF), FERTILIZATION-INDEPENDENT ENDOSPERM (FIE), RING1A/B, TERMINAL FLOWER 2 (TFL2), BMI1A/B, and EMBRYONIC FLOWER 2 (EMF2). We found that SUP interacts with CLF and TFL2 but not with the other proteins we tested (Appendix Fig S10A).

To define the region of SUP required for the interaction with CLF and TFL2, we tested a series of SUP truncations as baits with CLF and TFL2 AD fusion constructs. Full-length SUP was required for its interaction with CLF, while the interaction with TFL2 is mapped to a short region of the SUP protein (amino acids 89–205; Fig 5A and B). The EAR motif is essential for proper SUP function as an active repressor, and the ectopic expression of the truncated SUP protein without the EAR motif leads to *sup*-like floral phenotypes (Hiratsu *et al*, 2002). Thus, we also mutated the EAR motif in the full-length SUP protein and tested whether two versions of mutated SUP proteins (SUP-EARm1 and SUP-EARm2) interact with CLF and TFL2. The interaction of SUP with CLF but not with TFL2 requires the intact EAR motif (Fig 5A and B). These results suggest that the active repressor function of SUP could be more dependent on its interaction with CLF. To further verify the interactions of SUP with CLF and TFL2, we carried out a bimolecular fluorescence complementation (BiFC) assay in tobacco. Fluorescence was observed in the nuclei of tobacco epidermal cells only when SUP and CLF or when SUP and TFL2 constructs were co-infiltrated (Appendix Fig S10B). We further performed co-immunoprecipitation analysis to test the interaction between SUP and CLF *in vivo* (Fig 5C). To this end, we generated a functional *pCLF::HA-CLF* transgene and introgressed it into the *ap1 cal p35S::AP1-GR* background with or

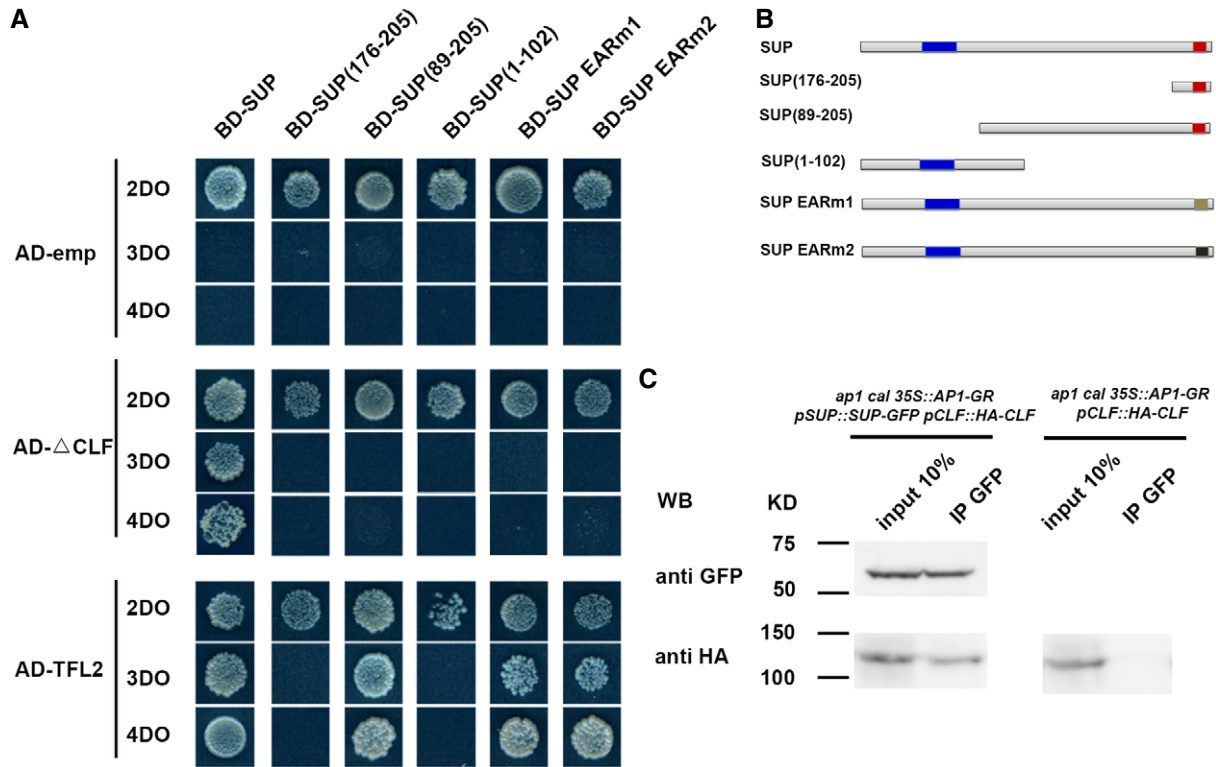


Figure 5. SUP interacts with PcG proteins CLF and TFL2.

A, B The yeast two-hybrid assay using a series of truncated SUP proteins with CLF and TFL2. Full-length, three truncated SUP proteins and SUP proteins with the two versions of the abolished EAR motif (EARM1 and EARM2) were fused to a GAL4 DNA-binding domain (BD). Schematic structures of the full-length, truncated, or mutated SUP protein are shown in (B). The blue region indicates the zinc finger domain; the red regions indicate an intact EAR motif; and beige and black regions indicate mutated EAR motif, respectively. The truncated CLF without its C-terminal SET domain (CLF) and the full-length TFL2 was fused to the GAL4 activation domain (AD). Yeast colonies harboring these fusion constructs and/or empty vectors as indicated were grown on selective media of 2DO, 3DO, and 4DO. For CLF, yeast growth was only detected when the combination of the full-length SUP and the truncated CLF was co-transformed. None of the truncated SUP proteins or SUP proteins with the mutated EAR motif interacted with the truncated CLF. For TFL2, a short domain of SUP (amino acids 89–205) was sufficient for the interaction, and the mutation of EAR motifs did not affect the interaction with TFL2.

C Interaction between SUP and CLF as determined by co-IP. Using stage 4 floral buds of *ap1 cal 35S::API-GR pSUP::SUP-GFP pCLF::HA-CLF* or of *ap1 cal 35S::API-GR pCLF::HA-CLF* plants, total proteins (input) were subjected to immunoprecipitation with anti-GFP-conjugated beads. Immunoblotting analysis with another anti-GFP and anti-HA antibody were performed to detect SUP-GFP (to test pull-down efficiency) and HA-CLF (protein interactions). Only in the samples containing both SUP-GFP and HA-CLF, HA-CLF was pull-down together with anti-GFP antibody. Molecular mass of the protein ladder is indicated in kilodaltons (KD).

Source data are available online for this figure.

without the *pSUP::SUP-GFP* transgene (Doyle & Amasino, 2009). We found that anti-GFP (recognizing SUP-GFP) could pull-down HA-CLF in stage 4 floral buds in *ap1 cal 35S::API-GR pSUP::SUP-GFP pCLF::HA-CLF*, but not in *ap1 cal 35S::API-GR pCLF::HA-CLF* (Fig 5C). Taken together, these results suggest that SUP can recruit the PcG complex to at least some of its target genes.

Discussion

WUS activity is essential for floral stem cell maintenance, and its termination at stage 6 is important to define the fixed number of whorls of floral organs (Lohmann et al, 2001). Delayed *WUS* termination in *ag* mutants leads to additional whorls of organs in the center of the flower (Bowman et al, 1991; Lenhard et al, 2001; Sun et al, 2009). The supernumerary whorls of stamens in *sup* mutant flowers suggest a possible delay of FM termination (Fig EV1; Gaiser

et al, 1995). *ag sup* double-mutant flowers show fasciated FMs, and extra petals continue to form in the center (Bowman et al, 1992; Breuil-Broyer et al, 2016), suggesting that SUP also has a spatial function in the regulation of FMs. In agreement with this assumption, increased numbers of stem cells (marked by the *pCLV3::GFP-ER*) were found in *sup-5* at floral stages 4–6 (Fig 1C–E), as compared to the wild type. Increased FM size in *sup* at late stage 5 was also confirmed with the meristem marker *pSTM::CFP-N7* (Fig EV2C and D). Prolonged *CLV3* and *STM* expressions in the center of the FM in *sup* (Figs EV1 and EV2) further show that the FM activity persists longer in *sup* than in wild type. Altogether, our data show that SUP affects floral stem cells both spatially and temporally.

There are two alternative but not mutually exclusive hypotheses to explain the increased number of stem cells in *sup*. Firstly, increased cell division rates could be responsible. A *sup* mutation did affect cell division rates at the whorl 3/4 boundary, as BrdU

incorporation assays showed reduced non-dividing domains at the boundaries between reproductive organs in both *sup-1* and *sup-5* flowers (Breuil-Broyer *et al.*, 2004, 2016). This increase in cell proliferation at the boundary regions in whorls 3 and 4 may explain the partial fusions between stamens and between stamens and carpels that are seen in *sup* (Breuil-Broyer *et al.*, 2004, 2016), but seem insufficient to explain the increase in stamen and carpel number. Indeed, we also observed that ectopic expression of *SUP* promotes the differentiation of the FM in the *clv3* background (Appendix Fig S9). Together with the expanded and prolonged expression of *CLV3* and *STM* in the FM of *sup* flowers (Figs 1, EV1 and EV2), this indicates that *SUP* promotes the differentiation of floral stem cells. Auxin affects cell division, and together with cytokinin, it also contributes to cell differentiation (Schaller *et al.*, 2015). Our work shows that *SUP* cell autonomously represses auxin biosynthesis, leading to a non-cell-autonomous effect in the center of the FM, with a depletion in auxin, as well as an increase in the number of floral stem cells and prolonged floral stem cell maintenance. We found that *SUP* directly represses the *YUC1/4* genes, reducing auxin biosynthesis at the whorl 3/4 boundary (Fig 4). We used different auxin reporters to compare auxin gradients in wild-type and *sup* flowers (expression patterns are summarized in Appendix Fig S11). Auxin is normally depleted at the boundary between whorls 3 and 4 (Fig 2C and D), where *SUP* is expressed, but strong auxin signaling is observed instead in this region when *SUP* is mutated (Fig 2A and B, and Appendix Fig S1A and B). Treatment of the anti-auxin PCIB and the analysis of IAM-treated *pSUP::iaaH* transgenic plants confirmed that increased auxin levels at the whorl 3/4 boundary are responsible for the floral indeterminacy in *sup* (Fig 2E–J). *SUP* was also shown to repress the expression of class B/stamen identity genes *AP3* and *PI* cell autonomously, but it remains unclear whether *AP3* and *PI* are direct targets of *SUP* (Prunet *et al.*, 2017). One possibility is that the local increase in auxin levels at the boundary between whorls 3 and 4 in *sup* flowers causes the ectopic expression of *AP3* and *PI*. Conversely, auxin levels appear lower in the center of the FM in *sup* flowers than in the wild type (Fig 2C and D), which is consistent with ectopic *CUC2* expression observed in the *sup* FMs (Fig EV3). The *PIN1* transporter generates an auxin flow toward regions with higher auxin levels (Schaller *et al.*, 2015), suggesting that increased auxin levels at the whorl 3/4 boundary in *sup* may cause auxin transport from the center of the FM to this neighboring boundary, resulting in auxin depletion at the center. Thus, changes in auxin dynamics based on polar transport may explain how *SUP* non-cell autonomously affects floral stem cells. Indeed, polar auxin transport also contributes to the formation of extra stamens and carpels in *sup*, as *NPA* treatments can partially rescue the *sup* phenotype (Appendix Fig S3). This suggests that up-regulation of local auxin biosynthesis at the whorl 3/4 boundary without polar auxin transport is not sufficient to cause the *sup* floral defects and that the extra auxin produced due to derepression of *YUC1/4* may trigger dynamic changes in auxin gradients in the FM through polar auxin transport. Interestingly, *PIN3* and *PIN4* were identified as potential downstream targets of *SUP*, and they appear down-regulated in a *sup* mutant background (Fig 3). However, we did not observe any obvious difference in *PIN3* localization between WT and *sup* flowers (Appendix Fig S9). Other polar auxin transporters might contribute to the changes in auxin distribution in the

center of *sup* mutant flowers. Both the cell-autonomous effect of *SUP* on auxin biosynthesis and class B gene expression at the boundary between whorls 3 and 4, and its non-cell-autonomous effect on auxin levels and stem cells in the center of the FM contribute to the control of stamen number. In *sup* mutant flowers, local derepression of auxin biosynthesis and class B gene expression allows for the formation of a few extra stamens at the boundary between whorls 3 and 4. This is not sufficient, however, to account for the large increase in stamen number in *sup* flowers. The *sup* phenotype is iterative: As these extra stamens emerge, they form a new boundary with the FM, and the lack of *SUP* function in this region causes the formation of more stamens. The increase in number and prolonged maintenance of floral stem cells replenishes the center of the FM and allows for several extra whorls of stamen to form.

The direct binding of *SUP* to the *YUC1* and *YUC4* loci, together with the ectopic expression of *YUC1* and *YUC4* at the boundary between whorls 3 and 4 in *sup* mutant flowers, suggests that both *YUC1* and *YUC4* are directly repressed by *SUP* in WT (Figs 4A–F and EV5A–D, and Appendix Fig S11). We also showed that both *yuc1* and *yuc4* mutant can partially rescue the abnormal stamen and carpel number in *sup*, and the *yuc1 yuc4* double mutant is epistatic to *sup-5* in flowers, confirming that *YUC1* and *YUC4* are major targets of *SUP*, and that their ectopic expression is responsible for the floral phenotype of *sup* (Fig 4G and H). Interestingly, we also found cytokinin-related genes among the potential targets of *SUP* (Appendix Table S1), suggesting that *SUP* function may involve a crosstalk between auxin and cytokinins.

Our yeast two-hybrid and BIFC assays revealed that both the PRC2 component *CLF*, which catalyzes H3K27 methylation (Goodrich *et al.*, 1997), and the PRC1 component *TFL2*, which interacts with the core catalytic components of the PRC1 complex, *AtRING1* and *AtBMI1* (Xu & Shen, 2008), associate with *SUP* (Fig 5 and Appendix Fig S10). We further validated the *SUP*-*CLF* interaction *in vivo* by co-IP assays (Fig 5C). Notably, *tfl2* mutants show similar developmental defects as *clf* plants (Goodrich *et al.*, 1997; Gaudin *et al.*, 2001). Moreover, *TFL2* was recently found to be a part of the PRC2 complex (Derkacheva *et al.*, 2013; Wang *et al.*, 2016). It will therefore be interesting to examine whether *TFL2* also participates in a *SUP*-*CLF*-containing complex. Yeast two-hybrid assays with *SUP* variants showed that the EAR motif, which is essential for the *SUP* repressor activity, is indispensable for *SUP*'s interaction with *CLF* (Fig 5A and B), indicating that the interaction between *CLF* and *SUP* is necessary for PRC2-mediated gene repression (Hiratsu *et al.*, 2002). Compared with *SUP*, the ubiquitously expressed *CLF* has a broader biological function in plant development and FM activity. *CLF* is involved in AG-mediated FM termination, and loss of function of *clf* has a weak FM indeterminacy (Liu *et al.*, 2011). In addition, *CLF* has multiple roles in flower development, including repression of *AG* and *STM*, and auxin signaling (Schubert *et al.*, 2006; Gu *et al.*, 2014). The derepression of *YUC1/4* in *sup* and the reduction in H3K27me3 level at the *YUC1/4* genomic regions suggest that *SUP* could function as the recruiter of *CLF*/*TFL2* to *YUC1/4* genomic regions (Figs 4A, C, D, and F, and EV5). It is worth noting that *SUP* can bind both the promoter and coding region of the *YUC1/4* and the coding region of *YUC1/4* is important for its negative transcription regulation (Fig 4A, B, D, and E, and

Appendix Fig S7). Recent genome-wide analysis with mutants of PRC1/2 components, including *clf* and *tfl2*, revealed that many transcription factors are associated with PRC2 target specificity in flower development, and both CLF and TFL2 are involved in spread of H3K27me3 marks (Wang et al, 2016). SUP contains a C2H2 zinc finger domain that is expected to bind DNA (Dathan et al, 2002). It is worth examining in the future whether SUP participates in the spreading of H3K27me3 marks at *YUC1/4* loci via this domain, and whether multiple DNA-binding motifs are required for SUP binding.

Materials and Methods

Plant materials and growth conditions

All *Arabidopsis thaliana* plants used were in the background of the Landsberg *erecta* (*Ler*) ecotype, except *clf-28*, *yuc1* (SALK_106293), *yuc4* (SALK_047083), and *pDR5rev::GFP*, which were from the Col-0 background and crossed into *Ler* at least three times. The *sup-1*, *sup-5*, *clf-28*, *wus-1*, *yuc1*, *yuc4*, *pCUC2::3xVENUS-N7*, *pCLV3::GFP-ER*, *pSTM::CFP-N7*, *pSUP-SUP-3xVenusN7*, *pDR5rev::GFP*, *pDR5rev::3xVENUS-N7*, *pRPS5A::DII-VENUS*, and *pDR5rev::2xGFP-N7* line were described previously (Bowman et al, 1989, 1992; Sakai et al, 1995; Laux et al, 1996; Goodrich et al, 1997; Heisler et al, 2005; Cheng et al, 2006; Xu et al, 2006a; Gordon et al, 2007; Doyle & Amasino, 2009; Landrein et al, 2015; Liao et al, 2015; Prunet et al, 2017). Plants were grown at 22°C under 24 h of continuous light. Genotyping primer sequences are shown in Appendix Table S2.

Chemical treatment and statistical analyses

For PCIB, NPA, and IAM treatments, *sup-5* or *pSUP::IAAH* and WT plants with inflorescence shoot of approximately 2 cm in length were dipped into concentrations of 100 μM, 100 μM, 100 μM, and 1 mM, respectively. Two open flowers from 10 individual plants (total of 20 flowers) were examined for the number of stamens and carpels on continuous days. Control mock treatments were performed using equal amounts of solvent and Silwet L-77. SEM was performed with flowers approximately 1 day before anthesis as previously described with minor changes (Xu et al, 2006b). Statistical significance was computed using Student's *t*-test.

Plasmid construction and plant transformation

For cloning, *pGreen-35S::SUP-GR* and *pGreen-pSUP::SUP-GFP* were prepared in a *pGreen* vector (www.addgene.org). *pENTR-pSUP::iaah* were prepared in a *pENTR/D-TOPO* vector (Invitrogen). The full length of genomic DNA of SUP of ~7.3 kb (−5,370 to +1,910) was cloned into a *pENTR* vector, and mutagenesis PCR was performed to introduce a SfoI site after the start codon. The IAAH fragment with the stop codon was then cloned into the SfoI site. GUS constructs were prepared using the Gateway system. Genomic DNA fragments were cloned into a *pENTR/D-TOPO* vector (Invitrogen) and recombined into *pBGFW* to fuse with the GUS coding region. *pYUC1::YUC1-GUS* contained a *YUC1* genomic region of

~4.8 kb (−2,904 to +1,904; A of the start codon was set as +1), while *pYUC1::GUS* only contained the promoter region (−2,904 to +10). *pYUC4::YUC4-GUS* was prepared with a *YUC4* genomic region of ~5.6 kb (−3,735 to +1,930; A of the start codon was set as +1), and *pYUC4::GUS* only contained the promoter region (−2,904 to +16). For *pCLF::HA-CLF*, the *CLF* genomic region of ~7.8 kb (−2,128 to +5,615) was cloned into a *pCR8/GW/TOPO* vector (Invitrogen). The SfoI restriction site was introduced just after ATG of *CLF* coding region by the mutagenesis PCR, and 3xHA was subcloned with the SfoI site. *pHGW* (Invitrogen) was used as the destination vector for *pCLF::HA-CLF*. Primer sequences are listed in Appendix Table S2. Transgenic plants were generated by floral dipping with *Agrobacterium tumefaciens* and the corresponding constructs. The additional *pSOUP* helper plasmid was co-transfected for the *pGreen*-based constructs during the transformation.

Microarray analysis

For inducible expression analysis with *p35S::SUP-GR*, a microarray analysis was performed with three biological replicates as described previously (Xu et al, 2013; Gan et al, 2014). The transgenic plants were grown at 22°C under 24-h light conditions. When the plants reached a height of around 5 cm, inflorescences containing flowers of up to stage 12 were harvested 4 h after the DEX or control mock treatment. Total RNAs were extracted using an RNeasy plant mini kit (Qiagen), and double-stranded cDNAs were synthesized with the Superscript Double-Stranded cDNA Synthesis Kit (Invitrogen). The microarray was performed according to NimbleGen's protocol (Roche). Gene expression was analyzed using Arraystar (DNAStar). Genes showing a 2.0-fold change in expression within a 90% confidence interval were considered to be differentially expressed and are presented in Appendix Table S3. Gene Ontology biological process enrichment was analyzed using agriGO software version 1.2 (<http://bioinfo.ca.u.edu.cn/agriGO/>). Enriched GO terms were further refined by REVIGO (<http://revigo.irb.hr/>) to reduce redundancy, with a cutoff of *P* < 0.01. The microarray data are available at the Gene Expression Omnibus (<https://www.ncbi.nlm.nih.gov/geo/>) under accession number GSE92729.

RNA extraction and expression analysis

To verify the microarray data, an inducible expression analysis with *p35S::SUP-GR* was performed with the transgenic inflorescences without open flowers harvested 2 and 4 h after the DEX or control mock treatments. To compare the expression profile between *sup* and WT, the inflorescences of *ap1-1 cal-1 p35S::API-GR sup-5* and *ap1-1 cal-1 p35S::API-GR* were harvested 3 days after 1 μM DEX treatment. Approximately 2 μg of total RNA was used for reverse transcription using the Superscript III RT-PCR system (Invitrogen). Real-time quantitative reverse transcription PCR was performed using an ABI PRISM 7900HT sequence detection system (Applied Biosystems) with KAPA SYBR FAST ABI Prism qPCR Master Mix (KAPA Biosystems). The ubiquitously expressed *Tip41-like* (*AT4G34270*; Czechowski et al, 2005) was used as an internal reference gene. Primer sequences are shown in Appendix Table S2.

GUS staining

For the GUS expression analysis, more than 20 independent T1 plants were obtained to examine the expression pattern (Sun *et al*, 2009). Inflorescences were incubated with GUS staining solution at 37°C overnight after the fixation in cold 90% acetone for 20 min, and the inflorescences were rinsed with GUS staining solution without X-Gluc. The resulting stained tissues were fixed with the fixative solution overnight before clearing by a series of ethanol solutions. The samples were then mounted on a microscope slide (Fisher) with one or two drops of Hoyer's clearing solution and observed under an Axio Scope A1 microscope (Zeiss).

Chromatin immunoprecipitation (ChIP) and co-immunoprecipitation (co-IP) assays

ChIP experiments were performed as previously described with minor modifications (Xu *et al*, 2013). Briefly, to investigate the SUP-GFP binding profiles at stage 4, total chromatin was extracted from *ap1-1 cal-1 p35S::API-GR sup-5 pSUP::SUP-GFP* inflorescences 3 days after 1 μM DEX treatment and immunoprecipitated using anti-GFP (Life Technologies, #A11122); normal rabbit IgG (Santa Cruz Biotechnology, #sc-2027) was used as the control. To investigate the epigenetic profile in *sup* mutants, total chromatin was extracted from *ap1-1 cal-1 p35S::API-GR sup-5* and *ap1-1 cal1-1 p35S::API-GR* inflorescences 3 days after 1 μM DEX treatment and immunoprecipitated using anti-H3K4me3 (Millipore, #07473) and anti-H3K27me3 (Millipore, #07449) anti-sera. DNA fragments were recovered with phenol–chloroform extraction and ethanol precipitation. Quantitative PCR with locus-specific primers (Appendix Table S2) was performed to measure the amounts of *YUC1* and *YUC4* fragments relative to those of the constitutively expressed *ACTIN2* (AT3G18780) on an ABI PRISM 7900HT sequence detection system (Applied Biosystems) using KAPA SYBR FAST ABI Prism qPCR Master Mix (KAPA Biosystems).

Co-immunoprecipitation was carried out as described previously with minor modification (Xu *et al*, 2014). The *pCLF::HA-CLF* was first transformed into the *clf-28* loss-of-function mutant. The transgenic plant of a single insertion, which can fully rescue *clf-28* mutant phenotype, was picked up and back-crossed into *Ler* three times. After that, *pCLF::HA-CLF* in *Ler* background was crossed into *ap1-1 cal-1 p35S::API-GR* with or without *pSUP::SUP-GFP*, respectively. Total proteins were extracted from inflorescences of *ap1-1 cal-1 p35S::API-GR pSUP::SUP-GFP pCLF::HA-CLF* or *ap1-1 cal-1 p35S::API-GR pCLF::HA-CLF* at 3 days after 1 μM DEX treatment, followed by immunoprecipitation with using anti-GFP (Life Technologies, #A11122). Immunoblotting was conducted to detect the presence of SUP-GFP (Santa Cruz Biotechnology, #SC-8334; 1:2,500 dilution) and CLF-HA (Santa Cruz Biotechnology, #SC-7392; 1:2,500 dilution) in the precipitate.

Yeast two-hybrid and bimolecular fluorescence complementation (BiFC) assay

For the yeast two-hybrid assay, the full-length coding sequences for *SUP*, *TFL2*, *RING1A/B*, *BMI1A/B*, *FIE*, *EMF2*, and the truncated CLF (without its C-terminal domain; according to Chanvivattana *et al*, 2004) were cloned in a Matchmaker GAL4 Two-Hybrid System 3

(BD Clontech) according to the manufacturer's instructions. Site mutagenesis and PCR were performed to mutate the functional amino acids of the EAR motif or to create a series of truncated SUP proteins. For the BiFC assay, the full-length coding sequences for *SUP*, *TFL2*, and the truncated *CLF* without its C-terminus were fused in frame with either the coding sequence for an N-terminal EYFP fragment or the C-terminal EYFP fragment of the primary pSAT1 vector (Lee *et al*, 2008). To detect the interaction in tobacco, leaves of 2- to 4-week-old tobacco plants were infiltrated with *Agrobacterium* containing the respective plasmid pairs (Sparkes *et al*, 2006). Epidermal cell layers were examined 3–4 days after infiltration and imaged with a Zeiss LSM 5 EXCITER upright laser scanning confocal microscope (Zeiss; Xu *et al*, 2013).

Measurements and image analysis

The images of the inflorescence with the *pSUP::SUP-3xVENUS* were taken with a Zeiss LSM 510 upright confocal microscope with a 40× oil objective, and the projections of confocal data were exported using Zeiss LSM software. All other confocal images were taken using a Leica SP8 confocal microscope with a 63× water-dipping objective or Zeiss LSM 710 and 780 with a 40× water-dipping objective as described previously (Prunet, 2017; Prunet *et al*, 2016), and cell measurements and image analyses were performed using the Imaris software (Bitplane).

Quantification of auxin

The inflorescences from *ap1-1 cal-1 p35S::API-GR sup-5* and *ap1-1 cal-1 p35S::API-GR* were harvested at 3 days after mock or 1 μM DEX treatment. Auxins were extracted and semi-purified as described previously (Kojima *et al*, 2009). IAA was quantified with ultra-high performance liquid chromatography (UHPLC)–electrospray interface (ESI) and quadrupole–orbitrap mass spectrometer (UHPLC/Q-Exactive™; Thermo Scientific) with an ODS column (AQUITY UPLC HSS T3, 1.8 μm, 2.1 × 100 mm; Waters; Shinozaki *et al*, 2015). Data collected from three biological replicates were analyzed by one-way ANOVA test.

Expanded View for this article is available online.

Acknowledgements

The authors would like to thank Jing Han Hong for reading the draft of this manuscript, Shen Lisha for the BiFC and Y2H constructs for some PcG components, and Jian Xu for the *pDRSrev::GFP* seeds and the unpublished transgenic plants that contain the *IAAH* gene. This work was supported by grants from the NAIST Foundation, the Mitsubishi Foundation, Grant-in-Aid for Scientific Research on Innovative Areas (Nos. 17H05843), Grant-in-Aid for Scientific Research A (No. 15H02405), Temasek Life Sciences Laboratory (TLL), and the National Research Foundation Singapore under the Competitive Research Programme (CRP Award NRF001-108) to T.I. Funding in the Meyerowitz Laboratory was provided by the Howard Hughes Medical Institute, the US National Institutes of Health through grant R01 GM104244, and the Gordon and Betty Moore Foundation through Grant GBMF3406. Funding in the Jack laboratory was provided by the US National Science Foundation through grant IOS-0926347. Funding in the Wellmer laboratory was provided by the Science Foundation Ireland through grant #10/IN.1/B2971.

Author contributions

YX and TI conceived the study. TI supervised and coordinated the study. YX, NP, EMM, and TI designed the experiments. YX and YW performed the Y2H, BiFC, and Co-IP assays. YX, NP, and TI prepared all the constructs and the transgenic lines. YX and NP took the confocal images. YX and E-SG carried out the microarray analysis and ChIP experiments. YX and NY carried out the genetic analysis. NY, YT, MK, TK, and HS quantified the auxin amount. YX and DS did transcriptional analysis. YX performed the SEM analysis. YX and JH performed the chemical treatments. YX, TI, NP, and EMM wrote the manuscript. TPJ and FW edited the manuscript. All authors discussed the results and approved the final manuscript.

Conflict of interest

The authors declare that they have no conflict of interest.

References

- Bowman JL, Smyth DR, Meyerowitz EM (1989) Genes directing flower development in *Arabidopsis*. *Plant Cell* 1: 37–52
- Bowman JL, Smyth DR, Meyerowitz EM (1991) Genetic interactions among floral homeotic genes of *Arabidopsis*. *Development* 112: 1–20
- Bowman JL, Sakai H, Jack T, Weigel D, Mayer U, Meyerowitz EM (1992) SUPERMAN, a regulator of floral homeotic genes in *Arabidopsis*. *Development* 114: 599–615
- Brand U, Fletcher JC, Hobe M, Meyerowitz EM, Simon R (2000) Dependence of stem cell fate in *Arabidopsis* on a feedback loop regulated by CLV3 activity. *Science* 289: 617–619
- Breuil-Broyer S, Morel P, de Almeida-Engler J, Coustham V, Negrutiu I, Trehin C (2004) High-resolution boundary analysis during *Arabidopsis thaliana* flower development. *Plant J* 38: 182–192
- Breuil-Broyer S, Trehin C, Morel P, Boltz V, Sun B, Chambrier P, Ito T, Negrutiu I (2016) Analysis of the *Arabidopsis* superman allelic series and the interactions with other genes demonstrate developmental robustness and joint specification of male-female boundary, flower meristem termination and carpel compartmentalization. *Ann Bot* 117: 905–923
- Chanvivattana Y, Bishopp A, Schubert D, Stoc C, Moon YH, Sung ZR, Goodrich J (2004) Interaction of Polycomb-group proteins controlling flowering in *Arabidopsis*. *Development* 131: 5263–5276
- Cheng Y, Dai X, Zhao Y (2006) Auxin biosynthesis by the YUCCA flavin monooxygenases controls the formation of floral organs and vascular tissues in *Arabidopsis*. *Genes Dev* 20: 1790–1799
- Clark SE, Running MP, Meyerowitz EM (1995) CLAVATA3 is a specific regulator of shoot and floral meristem development affecting the same processes as CLAVATA1. *Development* 121: 2057–2067
- Coen ES, Meyerowitz EM (1991) The war of the whorls: genetic interactions controlling flower development. *Nature* 353: 31–37
- Czechowski T, Stitt M, Altmann T, Udvardi MK, Scheible WR (2005) Genome-wide identification and testing of superior reference genes for transcript normalization in *Arabidopsis*. *Plant Physiol* 139: 5–17
- Daimon Y, Takabe K, Tasaka M (2003) The CUP-SHAPED COTYLEDON genes promote adventitious shoot formation on calli. *Plant Cell Physiol* 44: 113–121
- Dathan N, Zaccaro L, Esposito S, Isernia C, Omichinski JG, Riccio A, Pedone C, Di Blasio B, Fattorusso R, Pedone PV (2002) The *Arabidopsis* SUPERMAN protein is able to specifically bind DNA through its single Cys2-His2 zinc finger motif. *Nucleic Acids Res* 30: 4945–4951
- Dello Ioio R, Linhares FS, Scacchi E, Casamitjana-Martinez E, Heidstra R, Costantino P, Sabatini S (2007) Cytokinins determine *Arabidopsis* root-meristem size by controlling cell differentiation. *Curr Biol* 17: 678–682
- Derkacheva M, Steinbach Y, Wildhaber T, Mozgova I, Mahrez W, Nanni P, Bischof S, Gruissem W, Hennig L (2013) *Arabidopsis* MSI1 connects LHP1 to PRC2 complexes. *EMBO J* 32: 2073–2085
- Doyle MR, Amasino RM (2009) A single amino acid change in the enhancer of zeste ortholog CURLY LEAF results in vernalization-independent, rapid flowering in *Arabidopsis*. *Plant Physiol* 151: 1688–1697
- Fletcher JC, Brand U, Running MP, Simon R, Meyerowitz EM (1999) Signaling of cell fate decisions by CLAVATA3 in *Arabidopsis* shoot meristems. *Science* 283: 1911–1914
- Gaiser JC, Robinson-Beers K, Gasser CS (1995) The *Arabidopsis* SUPERMAN gene mediates asymmetric growth of the outer integument of ovules. *Plant Cell* 7: 333–345
- Gan ES, Xu Y, Wong JY, Goh JG, Sun B, Wee WY, Huang J, Ito T (2014) Jumonji demethylases moderate precocious flowering at elevated temperature via regulation of FLC in *Arabidopsis*. *Nat Commun* 5: 5098
- Gaudin V, Libault M, Pouteau S, Juul T, Zhao G, Lefebvre D, Grandjean O (2001) Mutations in LIKE HETEROCHROMATIN PROTEIN 1 affect flowering time and plant architecture in *Arabidopsis*. *Development* 128: 4847–4858
- Goodrich J, Puangsomlee P, Martin M, Long D, Meyerowitz EM, Coupland G (1997) A Polycomb-group gene regulates homeotic gene expression in *Arabidopsis*. *Nature* 386: 44–51
- Gordon SP, Heisler MG, Reddy GV, Ohno C, Das P, Meyerowitz EM (2007) Pattern formation during *de novo* assembly of the *Arabidopsis* shoot meristem. *Development* 134: 3539–3548
- Gordon SP, Chickarmane VS, Ohno C, Meyerowitz EM (2009) Multiple feedback loops through cytokinin signaling control stem cell number within the *Arabidopsis* shoot meristem. *Proc Natl Acad Sci USA* 106: 16529–16534
- Gu X, Xu T, He Y (2014) A histone H3 lysine-27 methyltransferase complex represses lateral root formation in *Arabidopsis thaliana*. *Mol Plant* 7: 977–988
- Heisler MG, Ohno C, Das P, Sieber P, Reddy GV, Long JA, Meyerowitz EM (2005) Patterns of auxin transport and gene expression during primordium development revealed by live imaging of the *Arabidopsis* inflorescence meristem. *Curr Biol* 15: 1899–1911
- Hiratsu K, Ohta M, Matsui K, Ohme-Takagi M (2002) The SUPERMAN protein is an active repressor whose carboxy-terminal repression domain is required for the development of normal flowers. *FEBS Lett* 514: 351–354
- Huang T, Lopez-Giraldez F, Townsend JP, Irish VF (2012) RBE controls microRNA164 expression to effect floral organogenesis. *Development* 139: 2161–2169
- Kojima M, Kamada-Nobusada T, Komatsu H, Takei K, Kuroha T, Mizutani M, Ashikari M, Ueguchi-Tanaka M, Matsuoka M, Suzuki K, Sakakibara H (2009) Highly sensitive and high-throughput analysis of plant hormones using MS-probe modification and liquid chromatography-tandem mass spectrometry: an application for hormone profiling in *Oryza sativa*. *Plant Cell Physiol* 50: 1201–1214
- Lafos M, Kroll P, Hohenstatt ML, Thorpe FL, Clarenz O, Schubert D (2011) Dynamic regulation of H3K27 trimethylation during *Arabidopsis* differentiation. *PLoS Genet* 7: e1002040
- Landrein B, Kiss A, Sassi M, Chauvet A, Das P, Cortizo M, Laufs P, Takeda S, Aida M, Traas J, Vernoux T, Boudaoud A, Hamant O (2015) Mechanical stress contributes to the expression of the STM homeobox gene in *Arabidopsis* shoot meristems. *Elife* 4: e07811

- Laux T, Mayer KF, Berger J, Jurgens G (1996) The WUSCHEL gene is required for shoot and floral meristem integrity in *Arabidopsis*. *Development* 122: 87–96
- Lee LY, Fang MJ, Kuang LY, Gelvin SB (2008) Vectors for multi-color bimolecular fluorescence complementation to investigate protein-protein interactions in living plant cells. *Plant Methods* 4: 24
- Leibfried A, To JP, Busch W, Stehling S, Kehle A, Demar M, Kieber JJ, Lohmann JU (2005) WUSCHEL controls meristem function by direct regulation of cytokinin-inducible response regulators. *Nature* 438: 1172–1175
- Lenhard M, Bohnert A, Jurgens G, Laux T (2001) Termination of stem cell maintenance in *Arabidopsis* floral meristems by interactions between WUSCHEL and AGAMOUS. *Cell* 105: 805–814
- Liao CY, Smet W, Brunoud G, Yoshida S, Vernoux T, Weijers D (2015) Reporters for sensitive and quantitative measurement of auxin response. *Nat Methods* 12: 207–210
- Liu X, Kim YJ, Muller R, Yumul RE, Liu C, Pan Y, Cao X, Goodrich J, Chen X (2011) AGAMOUS terminates floral stem cell maintenance in *Arabidopsis* by directly repressing WUSCHEL through recruitment of Polycomb Group proteins. *Plant Cell* 23: 3654–3670
- Lohmann JU, Hong RL, Hobe M, Busch MA, Parcy F, Simon R, Weigel D (2001) A molecular link between stem cell regulation and floral patterning in *Arabidopsis*. *Cell* 105: 793–803
- Meister RJ, Kotow LM, Gasser CS (2002) SUPERMAN attenuates positive INNER NO OUTER autoregulation to maintain polar development of *Arabidopsis* ovule outer integuments. *Development* 129: 4281–4289
- Nibau C, Di Stilio VS, Wu HM, Cheung AY (2011) *Arabidopsis* and Tobacco superman regulate hormone signalling and mediate cell proliferation and differentiation. *J Exp Bot* 62: 949–961
- Oka M, Miyamoto K, Okada K, Ueda J (1999) Auxin polar transport and flower formation in *Arabidopsis thaliana* transformed with indoleacetamide hydrolase (iaaH) gene. *Plant Cell Physiol* 40: 231–237
- Oono Y, Ooura C, Rahman A, Aspuria ET, Hayashi K, Tanaka A, Uchimiya H (2003) p-Chlorophenoxyisobutyric acid impairs auxin response in *Arabidopsis* root. *Plant Physiol* 133: 1135–1147
- Prunet N, Jack TP, Meyerowitz EM (2016) Live confocal imaging of *Arabidopsis* flower buds. *Dev Biol* 419: 114–120
- Prunet N (2017) Live confocal imaging of developing *Arabidopsis* flowers. *J Vis Exp* 122: e55156
- Prunet N, Yang W, Das P, Meyerowitz EM, Jack TP (2017) SUPERMAN prevents class B gene expression and promotes stem cell termination in the fourth whorl of *Arabidopsis thaliana* flowers. *Proc Natl Acad Sci USA* 114: 7166–7171
- Reddy GV, Meyerowitz EM (2005) Stem-cell homeostasis and growth dynamics can be uncoupled in the *Arabidopsis* shoot apex. *Science* 310: 663–667
- Sakai H, Medrano LJ, Meyerowitz EM (1995) Role of SUPERMAN in maintaining *Arabidopsis* floral whorl boundaries. *Nature* 378: 199–203
- Schaller GE, Bishopp A, Kieber JJ (2015) The yin-yang of hormones: cytokinin and auxin interactions in plant development. *Plant Cell* 27: 44–63
- Schubert D, Primavesi L, Bishopp A, Roberts G, Doonan J, Jenuwein T, Goodrich J (2006) Silencing by plant Polycomb-group genes requires dispersed trimethylation of histone H3 at lysine 27. *EMBO J* 25: 4638–4649
- Shinozaki Y, Hao S, Kojima M, Sakakibara H, Ozeki-Iida Y, Zheng Y, Fei Z, Zhong S, Giovannoni JJ, Rose JK, Okabe Y, Heta Y, Ezura H, Ariizumi T (2015) Ethylene suppresses tomato (*Solanum lycopersicum*) fruit set through modification of gibberellin metabolism. *Plant J* 83: 237–251
- Sparkes IA, Runions J, Kearns A, Hawes C (2006) Rapid, transient expression of fluorescent fusion proteins in tobacco plants and generation of stably transformed plants. *Nat Protoc* 1: 2019–2025
- Sun B, Xu Y, Ng KH, Ito T (2009) A timing mechanism for stem cell maintenance and differentiation in the *Arabidopsis* floral meristem. *Genes Dev* 23: 1791–1804
- Sun B, Looi LS, Gu S, He Z, Gan ES, Huang J, Xu Y, Wee WY, Ito T (2014) Timing mechanism dependent on cell division is invoked by Polycomb eviction in plant stem cells. *Science* 343: 1248559
- Supek F, Bosnjak M, Skunca N, Smuc T (2011) REVIGO summarizes and visualizes long lists of gene ontology terms. *PLoS One* 6: e21800
- Takada S, Hibara K, Ishida T, Tasaka M (2001) The CUP-SHAPED COTYLEDON1 gene of *Arabidopsis* regulates shoot apical meristem formation. *Development* 128: 1127–1135
- Uemura A, Yamaguchi N, Xu Y, Wee W, Ichihashi Y, Suzuki T, Shibata A, Shirasu K, Ito T (2017) Regulation of floral meristem activity through the interaction of AGAMOUS, SUPERMAN, and CLAVATA3 in *Arabidopsis*. *Plant Reprod* 31: 89–105
- Wang H, Liu C, Cheng J, Liu J, Zhang L, He C, Shen WH, Jin H, Xu L, Zhang Y (2016) *Arabidopsis* flower and embryo developmental genes are repressed in seedlings by different combinations of polycomb group proteins in association with distinct sets of cis-regulatory elements. *PLoS Genet* 12: e1005771
- Wellmer F, Alves-Ferreira M, Dubois A, Riechmann JL, Meyerowitz EM (2006) Genome-wide analysis of gene expression during early *Arabidopsis* flower development. *PLoS Genet* 2: e117
- Werner T, Motyka V, Laucou V, Smets R, Van Onckelen H, Schmulling T (2003) Cytokinin-deficient transgenic *Arabidopsis* plants show multiple developmental alterations indicating opposite functions of cytokinins in the regulation of shoot and root meristem activity. *Plant Cell* 15: 2532–2550
- Xu J, Hofhuis H, Heidstra R, Sauer M, Friml J, Scheres B (2006a) A molecular framework for plant regeneration. *Science* 311: 385–388
- Xu Y, Teo LL, Zhou J, Kumar PP, Yu H (2006b) Floral organ identity genes in the orchid *Dendrobium crumenatum*. *Plant J* 46: 54–68
- Xu L, Shen WH (2008) Polycomb silencing of KNOX genes confines shoot stem cell niches in *Arabidopsis*. *Curr Biol* 18: 1966–1971
- Xu Y, Wang Y, Stroud H, Gu X, Sun B, Gan ES, Ng KH, Jacobsen SE, He Y, Ito T (2013) A matrix protein silences transposons and repeats through interaction with retinoblastoma-associated proteins. *Curr Biol* 23: 345–350
- Xu Y, Gan ES, Zhou J, Wee WY, Zhang X, Ito T (2014) *Arabidopsis* MRG domain proteins bridge two histone modifications to elevate expression of flowering genes. *Nucleic Acids Res* 42: 10960–10974
- Yamaguchi N, Huang J, Xu Y, Tanoi K, Ito T (2017) Fine-tuning of auxin homeostasis governs the transition from floral stem cell maintenance to gynoecium formation. *Nat Commun* 8: 1125
- Yun JY, Weigel D, Lee I (2002) Ectopic expression of SUPERMAN suppresses development of petals and stamens. *Plant Cell Physiol* 43: 52–57
- Zadnikova P, Simon R (2014) How boundaries control plant development. *Curr Opin Plant Biol* 17: 116–125
- Zhao Z, Andersen SU, Ljung K, Dolezal K, Miotk A, Schultheiss SJ, Lohmann JU (2010) Hormonal control of the shoot stem-cell niche. *Nature* 465: 1089–1092